

Convolution-based Soma Counting Algorithm for Confocal Microscopy Image Stacks

Shih-Ting Huang, Yue Jiang and Hao-Chiang Shao ^a

Department of Statistics and Information Science, Fu Jen Catholic University, Taiwan, Republic of China

Keywords: Neuroblast, Soma Detection, *Drosophila* Brain, Confocal Microscopy.

Abstract: To facilitate brain research, scientists need to identify factors that can promote or suppress neural cell differentiation mechanisms. Accordingly, the way to recognize, segment, and count developing neural cells within a microscope image stack becomes a fundamental yet considerable issue. However, it is currently not feasible to develop a DCNN (deep convolutional neural network) based segmentation algorithm for confocal fluorescence image stacks because of the lack of manual-annotated segmentation ground truth. Also, such tasks traditionally require meticulous manual preprocessing steps, and such manual steps make the results unstable even with software support like ImageJ. To solve this problem, we propose in this paper a convolution-based algorithm for cell recognizing and counting. The proposed method is computationally efficient and nearly parameter-free. For a $1024 \times 1024 \times 70$ two-channel image volume containing about 100 developing neuron cells, our method can finish the recognition and counting tasks within 250 seconds with a standard deviation smaller than 4 comparing with manual cell-counting results.

1 INTRODUCTION

Biological labs need to identify factors, including gene fragments, that can promote or suppress neural cell differentiation mechanisms to facilitate brain research. To understand the impact of the transplanted gene fragment on neurodevelopment, the difference of the number of neural cells between the wild type, i.e., the phenotype of the typical form of a species as it occurs in nature, and a mutant, i.e., the individual with transplanted RNA interference fragments, should be clarified. Hence, the way to recognize, segment, and count developing neural cells within a microscope image volume becomes a fundamental yet considerable issue. However, it is currently not feasible to segment these kinds of confocal fluorescence image volumes by using convolutional neural networks (CNN), such as U-Net (Ronneberger et al., 2015) or 3D U-Net (Çiçek et al., 2016), because of i) the lack of labeled segmentation ground truth and ii) the oversized confocal image volumes. Also, such tasks traditionally require meticulous manual steps, so the results cannot be stable even with software support like ImageJ (Ima, 2020). To settle down this problem, we propose in this paper an algorithm for

cell recognizing and counting based on convolutional operators and conventional image processing skills. The proposed method is computationally efficient, nearly parameter-free, and aims to extract trustworthy segmentation ground truth for developing advanced CNN-based algorithms. For a $1024 \times 1024 \times 70$ focal stack, focused on the calyx of the mushroom body in the *Drosophila* brain, containing about 100 developing neuron cells, our method can finish the recognition and counting tasks within 240 seconds with a standard deviation smaller than 4 comparing with the manual cell-counting results. To process this kind of confocal image volume, the current standard is still a computer-aided manual procedure, for instance, using common software including ImageJ (Ima, 2020) and Imaris (ima, 2020). However, these programs require manual input, and therefore they cannot provide reliable results if the user does not have sufficient anatomical knowledge of the fly brain and neurons. In addition, because for confocal microscopy imaging the sampling interval on the z -axis is usually three times the sampling interval on the x - and the y -axes, it is difficult and time-consuming to clarify the relationship between soma candidates on adjacent slices. Therefore, we proposed this method to segment and count neuroblast cells.

^a  <https://orcid.org/0000-0002-3749-234X>

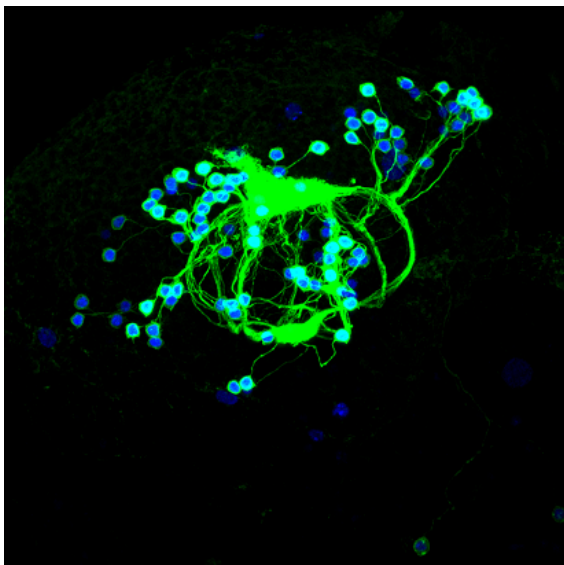


Figure 1: Maximum intensity projection (MIP) of an example confocal fluorescence image volume. Red balls are neuron cell bodies (soma), green channel records neural fibres and cell membranes, and dark red areas are background tissues of fly brain. Note that in order to avoid confusion in red and green channels, we illustrate all MIP images by swapping blue and red channels later in this paper. Note that in this figure we render the RED channel in blue so that even color-blind readers can distinguish soma from neural fibers and membranes.

2 RELATED WORK

To process 2D+Z confocal fluorescence image volumes, several methods were proposed. However, most of them focus on image atlasing and surface registration (Chen et al., 2012; Shao et al., 2013; Shao et al., 2014), a few of them describe segmentation strategies on neuron fibers and neuropils (Shao et al., ; Shao et al., 2019), but none of them depicts soma (cell body) identification methods. Although in (Shao et al.,) Shao et al. trace neural fibers within a brainbow/flybow (Livet et al., 2007; Hadjiconomou et al., 2011) image volume by identifying soma candidates first (Shao et al.,), their method lacks a mechanism to rule out false somas so that it is hard for their method to separate independent neurons. In addition, Shao and his co-authors also stated in (Shao et al., 2011) and (Shao et al.,) that the effectiveness of image processing routines designed for confocal fluorescence images may be degraded due to fluorescence halation. The pin-hole of the confocal microscope still cannot filter out fluorescence emitted from out-of-focus planes. Hence, some anti-halation methods are still necessary for confocal imagery. To remove halation, Shao et al. adopted morphological top-hat

transform in (Shao et al.,). However, this strategy requires a pre-defined marker and a suitable structural element, so it cannot be robust. Therefore, we finally decided to utilize the common most deconvolution method, i.e., Lucy-Richardson deconvolution (Fish et al., 1995), to remove all possible fluorescence halation due to the imaging point spread function. In next section, we will describe our method in detail.

3 METHOD

3.1 Overview

A common strategy to detect neuron cell bodies is to use morphological operations, i.e., erosion and dilation with handcrafted structural elements, as reported in (Shao et al.,). However, such a strategy is not robust against noises and therefore needs several post-processing steps to rule out unqualified candidates of neuron cell bodies.

The proposed method was designed for two purposes. First, this method was developed to provide a cell-body identification result that is more stable than those obtained by manual procedures. Second, this method was developed to mass-produce cell body segmentation results for a further study like training and specializing in a U-net for this application. Therefore, the proposed method was designed and implemented by using primarily convolutional operations.

3.2 Soma Identifier

To systematically extract neuron cell bodies (soma), we first derive several $W \times H \times Z$ feature maps by convoluting source image volume with several 2D+Z Gaussian kernels of different σ_i and window size w_i . Practically, each Gaussian kernel is a 3D array with its entries specified by following equations.

$$\mathcal{F}_i = I * G_i(\sigma_i, w_i), \quad (1)$$

where $*$ denotes 3D convolution, and G_i is a $w_i \times w_i$ convolution kernel with entries defined by

$$G_i = \alpha e^{-\mathbf{X}^T \mathbf{X} / \sigma_i^2} \text{ with } \mathbf{X}^T = (x, y, 3z). \quad (2)$$

Here, I is the source image volume, \mathcal{F}_i is the feature map corresponding to the i^{th} Gaussian convolution kernel $G(\sigma_i, w_i)$, and α denotes a constant gain factor used to normalize G_i . Note that the factor 3 in Eq. (2) reflects the sampling interval in the z axis, as we will describe in Section 4.1.

The aforementioned convolution step can be regarded as a template matching process. Consequently,

we can find candidates of neuron cell bodies by identifying local maximums on all feature map \mathcal{F}_i . By letting $\delta_i(j)$ denote the list recording the j^{th} local maximum of feature map \mathcal{F}_i , this second step aims to find the intersection set of local maximums of all feature maps. We use Δ_{main} to denote the resulting intersection set, that is,

$$\Delta_{main} = \cap_i \delta_i. \quad (3)$$

3.3 Halation Suppression

However, neurons cell bodies may be locally-concentrated near specific neuropils; in this situation, for example, two close neuron cell bodies would be entangled on microscopy images and thus usually result in one ridge, rather than two local maximums, on the feature map. To overcome this difficulty, we apply Richardson–Lucy deconvolution (Richardson, 1972) method to remove the effect of halation in the fluorescence image volume so that neuron cell bodies, which cluster within a small region, becomes distinguishable. Then, we repeat the **Soma identifier** procedure described in previous subsection by utilizing smaller convolution kernels, denoted as $G_{psf}(\sigma_{psf}, w_{psf})$, and then detect the local maximums to find cell bodies candidates again. We use Δ_{aux} to denote Cell bodies detected in this stage. Note that Richardson–Lucy deconvolution method requires a user-specified blur kernel, i.e., the point spread function (PSF); in our implementation, the blur kernel used in this step is also the convolution kernel $G_{psf}(\sigma_{psf}, w_{psf})$.

Because Richardson–Lucy deconvolution may enhance/highlight imaging noise, fake cell body candidates would be produced after the second convolutional detection procedure. To settle this issue, we collect experiment results of more than 80 confocal image volumes, each acquired with different sample preparation condition and imaging configurations, and then induce following judgement rules.

- For any two cell body candidates, if the distance between them is no larger than 10 voxels, we rule out the one with lower average brightness.
- If a new cell body candidate (derived in the second step) does not locate within the bounding box of any soma candidate obtained in the first step, we will disregard it unless its average brightness reaches level of top 1%.

Finally, because we now have only about 80 image volumes of different geno-types and different imaging parameter settings, all above rules are developed empirically. We will show our experiment result in next section.

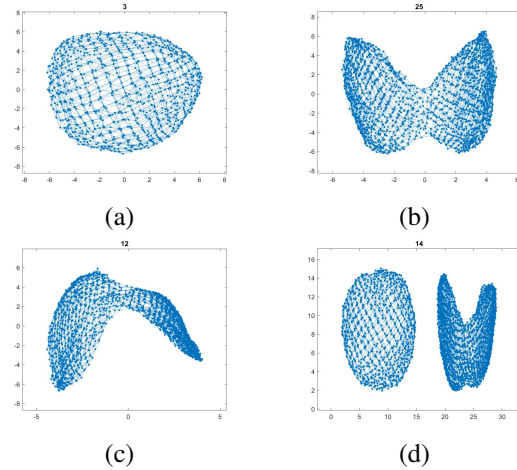


Figure 2: Visualized graph of different soma candidates. (a) a typical graph showing only one soma; (b) a graph showing two concatenated soma; (c) one another example of two concatenated soma; and, (d) a local graph showing there are three soma within this area.

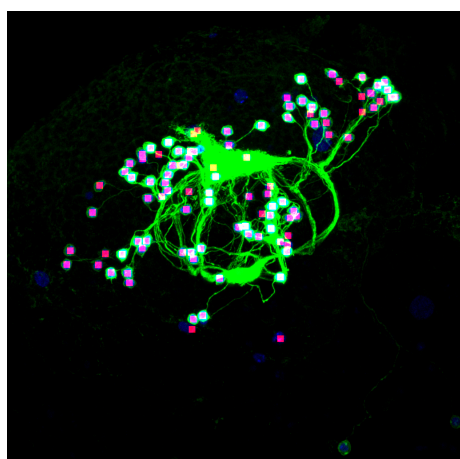
3.4 Graph Reconstruction for Manual Validation

This step is optional in our design; and, it will be applied if the number of neural cell bodies in the left brain and that in the right brain are too different. In this step, we reconstruct and visualize a graph model for pixels of each extracted soma, and this visualization can at least assist users to verify if there are multiple neural cell bodies within an “extracted soma”. Demonstrated in Figure 2 are examples of visualized graphs. Note that these are K-nearest-neighbor (kNN) graphs derived by taking each pixel’s (x, y, z, intensity) information into account. Through this representation, we can validate the effective number of somas within “one soma candidate”, predicted by our algorithm, efficiently.

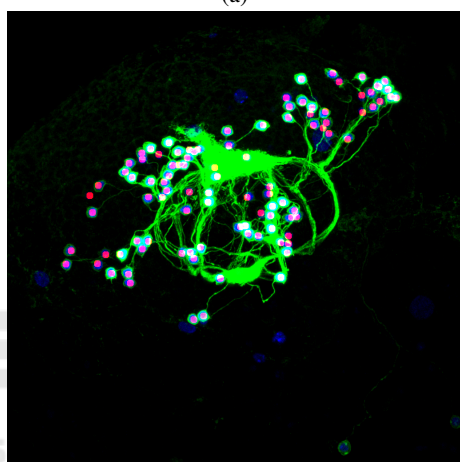
4 EXPERIMENT RESULT

4.1 Dataset

All source image volumes used in this paper were acquired by an LSM-700 confocal microscope. Each image volume contains two channels. The red channel records fluorescence emitted by neuron cell bodies by using the excitation laser at 555 nm, and the green channel records neuron cell membrane and neuron fibers by using the excitation laser at 488 nm. The spatial dimension of all image volumes is $1,024 \times 1,024$, and an image volume may contain about 50 ~ 100



(a)



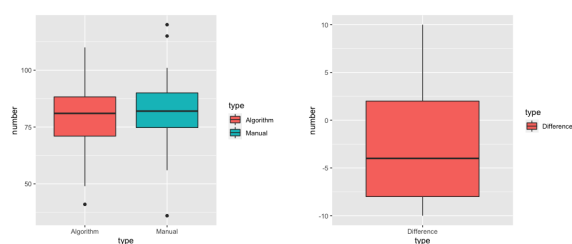
(b)

Figure 3: Comparison between MIP images of (a) our result and (b) the manual labeling result of the image volume shown in Figure 1. The source image volume contains 100 slices.

slices. Note that the actual size of each voxel is about $0.16 \times 0.16 \times 0.50 \mu\text{m}^3$.

4.2 Discussion

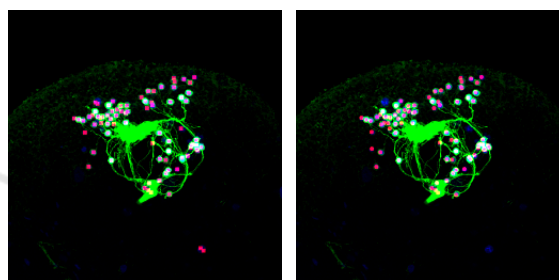
Because there is not state-of-the-art or benchmark method in this field, we compare our segmentation results with manual counting/labeling results. Figure 3 shows the comparison among the MIP image of one source volume, the MIP image of our soma identification result, and the MIP image of manual labeling result. Here, red balls are neural cells, green channel records neural fibres and cell membranes, and dark red areas are background tissues of fly brain. Note that we changed the source red-channel that records neuron cell bodies to the blue-channel so that even readers with color-vision-deficiency can read our illustrations. Also, summarized in Figure 4 is the sta-



(a)

(b)

Figure 4: Statistical comparison. (a) This plot shows that the average number of extracted soma of the proposed method is almost the same with that of manual counting result. (b) This plot shows that the difference between our segmentation result and manual ground truth mostly ranging from -7.5 to 2.5.



(a)

(b)

Figure 5: Comparison between MIP images of the manual labeling result and our result. This source image volume contains 82 slices. (a) Result derived by our method. (b) Manual labelling result.

tistical information of our experiment soma counting results. Finally, shown in Figures 5 ~ 9 are results of other five image volumes.

These experiment results prove that the proposed method can provide much more stable and reliable soma counting results than manual process. However, the proposed method now has two obvious drawbacks. First, it may misrecognizes other cells as neuroblasts once they were labeled by the antibody during the stain process. Second, for image volumes with low brightness, several neuron cell bodies may be disregarded because their voxel intensities are too weak to hold their contour shape.

5 CONCLUDING REMARKS

In this paper, we proposed a cell-counting prototype algorithm for confocal fluorescence image volumes. Compared with time-consuming manual and software-assisted cell-counting strategies, the proposed method can finish the calculation of a $1024 \times 1024 \times 80$ image volume within 5 minutes and provide a better and more stable segmentation and count-

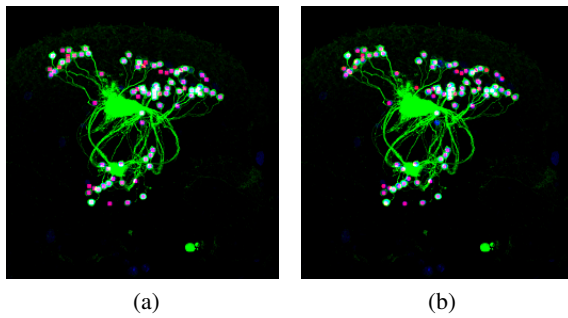


Figure 6: Comparison between MIP images of the manual labeling result and our result. This source image volume contains 83 slices. (a) Result derived by our method. (b) Manual labelling result.

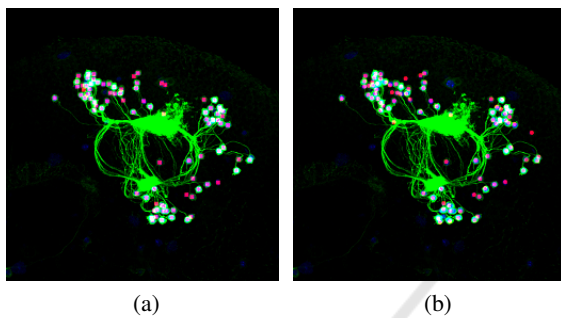


Figure 7: Comparison between MIP images of the manual labeling result and our result. This source image volume contains 89 slices. (a) Result derived by our method. (b) Manual labelling result.

ing result. The proposed method has one primary limitation. That is, for flat, disc-shaped neuron cell bodies, especially those with extra-low brightness and existing on less than three slices, the proposed algorithm may fail to recognize them.

The proposed algorithm currently may also fail to recognize flat and disc-shaped cells, especially those that only exist on less than three slices. We are currently working on this issue. Also, as for the neuro-

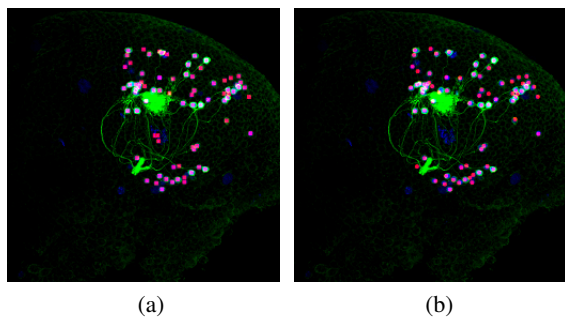


Figure 8: Comparison between MIP images of the manual labeling result and our result. This source image volume of a wide-type contains 76 slices. (a) Result derived by our method. (b) Manual labelling result.

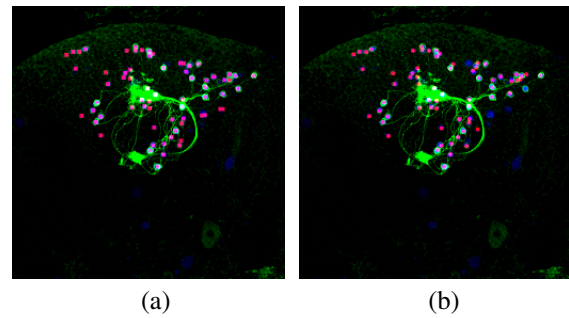


Figure 9: Comparison between MIP images of the manual labeling result and our result. This source image volume of a wild-type contains 67 slices. (a) Result derived by our method. (b) Manual labelling result.

last in *Drosophila* brain, there is still one another sample preparation method, which is designed for imaging tissue in a very large field of view but labeling neuron cell membrane only. Hence, one of our future extensions is to modify our prototype algorithm for this kind of image.

ACKNOWLEDGEMENT

This work supported by MOST 107-2320-B-030-012-MY3. The authors want to thank Prof. Hung-Hsiang Yu from the Institute of Cellular and Organismic Biology, Academia Sinica, Taiwan for providing the source confocal microscopy image volumes.

REFERENCES

- (2020). Imagej. <https://imagej.nih.gov/ij/>.
- (2020). Imaris. <https://imaris.oxinst.com/>.
- Chen, G.-Y., Wu, C.-C., Shao, H.-C., Chang, H.-M., Chiang, A.-S., and Chen, Y.-C. (2012). Retention of features on a mapped drosophila brain surface using a bezier-tube-based surface model averaging technique. *IEEE transactions on biomedical engineering*, 59(12):3314–3326.
- Çiçek, Ö., Abdulkadir, A., Lienkamp, S. S., Brox, T., and Ronneberger, O. (2016). 3d u-net: learning dense volumetric segmentation from sparse annotation. In *International conf. on medical image computing and computer-assisted intervention*, pages 424–432. Springer.
- Fish, D., Brinicombe, A., Pike, E., and Walker, J. (1995). Blind deconvolution by means of the richardson-lucy algorithm. *JOSA A*, 12(1):58–65.
- Hadjieconomou, D., Rotkopf, S., Alexandre, C., Bell, D. M., Dickson, B. J., and Salecker, I. (2011). Flybow: genetic multicolor cell labeling for neural circuit analysis in drosophila melanogaster. *Nature methods*, 8(3):260–266.

- Livet, J., Weissman, T. A., Kang, H., Draft, R. W., Lu, J., Bennis, R. A., Sanes, J. R., and Lichtman, J. W. (2007). Transgenic strategies for combinatorial expression of fluorescent proteins in the nervous system. *Nature*, 450(7166):56–62.
- Richardson, W. H. (1972). Bayesian-based iterative method of image restoration. *JoSA*, 62(1):55–59.
- Ronneberger, O., Fischer, P., and Brox, T. (2015). U-net: Convolutional networks for biomedical image segmentation. In *International Conference on Medical image computing and computer-assisted intervention*, pages 234–241. Springer.
- Shao, H.-C., Cheng, W.-Y., Chen, Y.-C., and Hwang, W.-L. Colored multi-neuron image processing for segmenting and tracing neural circuits. In *2012 19th IEEE International Conference on Image Processing*, pages 2025–2028. IEEE.
- Shao, H.-C., Hwang, W.-L., and Chen, Y.-C. (2011). Optimal multiresolution blending of confocal microscope images. *IEEE transactions on biomedical engineering*, 59(2):531–541.
- Shao, H.-C., Wang, Y.-M., and Chen, Y.-C. (2019). A two-phase segmentation method for drosophila olfactory glomeruli. In *2019 IEEE International Conf. on Image Processing (ICIP)*, pages 265–269. IEEE.
- Shao, H.-C., Wu, C.-C., Chen, G.-Y., Chang, H.-M., Chiang, A.-S., and Chen, Y.-C. (2014). Developing a stereotypical drosophila brain atlas. *IEEE Transactions on Biomedical Engineering*, 61(12):2848–2858.
- Shao, H.-C., Wu, C.-C., Hsu, L.-H., Hwang, W.-L., and Chen, Y.-C. (2013). 3d thin-plate spline registration for drosophila brain surface model. In *2013 IEEE International Conf. on Image Processing*, pages 1438–1442. IEEE.